Analysis of early cellular responses of anterior cruciate ligament fibroblasts seeded on different molecular weight polycaprolactone films functionalized by a bioactive poly(sodium styrene sulfonate) polymer

Amélie Leroux,[1] Jagadeesh K. Venkatesan,[2] David G. Castner,[3] Magali Cucchiarini,[2] and Véronique Migonney[1,a)]

[1]*Laboratory of Biomaterials and Polymers of Specialty, Institut Galilée, Université Paris 13, Sorbonne Paris Cité, UMR CNRS 7244, 93430 Villetaneuse, France*

[2]*Center of Experimental Orthopaedics, Saarland, University Medical Center and Saarland University, D-66421 Homburg/Saar, Germany*

[3]*National ESCA and Surface Analysis Center for Biomedical Problems (NESAC/Bio), Department of Bioengineering and Department of Chemical Engineering, University of Washington, Box 351653, Seattle, Washington 98195*

(Received 24 April 2019; accepted 22 July 2019; published 12 August 2019)

With the growing number of anterior cruciate ligament (ACL) ruptures and the increased interest for regenerative medicine procedures, many studies are now concentrated on developing bioactive and biodegradable synthetic ligaments. For this application, the choice of raw materials with appropriate physicochemical characteristics and long-term degradation features is essential. Polycaprolactone (PCL) has the advantage of slow degradation that depends on its molecular weight. This study evaluates two PCL materials: a technical grade (PC60: 60 kDa) versus a medical grade (PC12: 80 kDa), both before and after functionalization with poly(sodium styrene sulfonate) (pNaSS). After determining the grafting process had little to no effect on the PCL physicochemical properties, sheep ACL fibroblast responses were investigated. The PC12 films induced a significantly lower expression of the tumor necrosis factor alpha inflammatory gene compared to the PC60 films. Both film types induced an overproduction of fibroblast growth factor-2 and transforming growth factor beta compared to the controls on day 5 and demonstrated collagen gene expression profiles similar to the controls on day 7. Upon protein adsorption, pNaSS grafting caused a rapid cell adhesion in the first 30 min and an increased adhesion strength (1.5-fold higher). Moreover, after 7 days, an increase in cell density and actin network development were noted on the grafted films. *Published by the AVS.* https://doi.org/10.1116/1.5102150

I. INTRODUCTION

With one person out of 3000 in the United States affected (i.e., 120 000 surgical reconstructions per year), the anterior cruciate ligament (ACL) is one of the most commonly injured ligaments of the knee.[1] In addition to the pain associated with the ACL rupture, patients have to face long-term consequences such as a decrease in their sports activity level, a high risk of recurrence and clinical sequelae including meniscal tears, chondral lesions, and an increased risk of early post-traumatic osteoarthritis.[2] Currently, when a ligament surgical intervention is needed, the gold standard is the autograft. However, this technique requires taking a graft from a different anatomic area, which increases the operative time and may lead to morbidity at the sampling site.[3]

With an increase in ACL ruptures in recent decades, especially in women,[4] and in light of the availability of tissue engineering procedures, there has been a growing research focus on the development of biodegradable synthetic ligaments.[5–10] The main objective of the present study was to create a biodegradable structure supporting the ligament functions that allow for neoligament formation. To achieve this goal, we used polycaprolactone (PCL), a long-term degradable, semicrystalline polymer with a glass transition temperature (T_g) of −60 °C and a melting temperature (T_f) of 59–64 °C that depends on crystallinity.[11] Thus, PCL is an easily workable material at relatively low temperatures and its crystallinity may be modulated upon shaping treatments. Furthermore, its degradation rate is correlated to its molecular weight and can be up to four years. The number average molecular weight (M_n) of PCL structures generally ranges from 3000 to 80 000 g/mol.[11] Consequently, several raw PCLs are available and a multitude of final constructs can be produced in terms of physicochemical features. For development of a new prosthesis, the choice and the characterization of the polymer used are essential. With the aim of selecting a PCL with the required properties for the ligament reconstruction application, we assessed in parallel a well-characterized, commercial PCL and a medical grade PCL.

In addition, to faster recreate a neoligament and increase the bioactivity of a synthetic material, many researchers use surface modification. Two common approaches are used: (i) coating or (ii) chemical modification of the surface. Regardless of the method of surface treatment employed, the choice of the species used to modify the surface is crucial. Some scientists seek to directly immobilize extracellular

a)Author to whom correspondence should be addressed: veronique.migonney@univ-paris13.fr

matrix (ECM) proteins such as fibronectin (Fn) and hyaluronic acid onto the surface,[5,12,13] some immobilize just specific amino acid sequences such as Tripeptide Arginin, Glycin, Aspartic acid (Refs. 14 and 15) and some immobilize synthetic biomolecules.[16–18] With the aim of ligament reconstruction and to build on an already developed bioactive synthetic ligament,[19–21] the current study focused on the functionalization of PCL surfaces with poly(sodium styrene sulfonate) (pNaSS), a bioactive polymer that has been shown[16–25] to endow surfaces with bioactive properties such as the modulation of adhesive protein conformations, the modulation of cell and bacteria adhesion, and the improvement of *in vivo* biointegration.

While previous studies emphasized the biological impact either of different physicochemical features of the surface, such as the crystallinity,[26] or of the bioactive effect of a specific molecule,[27] few considered jointly these two aspects. To choose the best PCL raw material coupled with a bioactive molecule for the ligament regeneration, we evaluated the early cellular responses of ACL fibroblasts seeded onto two different molecular weight PCL films with or without pNaSS functionalization. Two PCL materials were studied: one technical grade with a lower molecular weight and one medical grade with a higher molecular weight. Both were successfully grafted with pNaSS. We hypothesized that the grafting did not impact the physicochemical characteristics of PCL. Biologic responses including cytotoxicity, proliferation, morphology, growth factor production, gene expression, and cell adhesion were studied. To generate a new ligament, a synthetic prosthesis will likely need to promote ECM synthesis. Therefore, we examined the production of the basic fibroblast growth factor (FGF-2) and transforming growth factor beta (TGF-β) for their pro-anabolic activities of collagen production,[28] especially type-I and type-III collagen.[29] Potential inflammatory responses to the materials were also monitored by investigating the tumor necrosis factor alpha (TNF-α) gene expression profiles. We tested the hypothesis that the medical grade material generated optimal cellular responses. The pNaSS grafting is expected to favor cell activities. Finally, cell adhesion assays were performed to evaluate the working mechanism of this bioactive polymer.

II. MATERIALS AND METHODS

A. Sample preparation

1. PCL film spin-coating

Two different types of PCL films were cast by spin-coating. Raw PCL pellets either from Sigma-Aldrich (St Quentin Fallavier, France) (sku 704105, i.e., PC60) or from Corbion (Amsterdam, The Netherlands) (sku Purasorb PC12, medical grade) were dissolved in a dichloromethane solution (30%, w/v) under stirring for several hours. When the viscous solution became homogeneous, it was dropped onto a glass slide and then spun for 30 s either at 1500 rpm (PC60 films) or at 1000 rpm (PC12 films) using an SPIN150-v3 SPS. The shaped films were dried overnight at air pressure and room temperature for natural evaporation of the solvent. Using a punch, the cast films were cut into smaller pieces of 14-mm diameter and then stored at 4 °C until further experiments.

2. Grafting of pNaSS on PCL films

a. Purification of the NaSS monomer. Sodium 4-vinylbenzenesulfonate salt (NaSS, sku 94904, Sigma-Aldrich) was purified by recrystallization in an ethanol-distilled water solution (90:10, v:v). Typically, 90 g of NaSS was dissolved overnight in 1780 ml of the mixed solvent at 70 °C. The mixture was then filtrated and the filtrate stored at 4 °C for 48 h. After final filtration, the filter cake (recrystallized NaSS) was collected, vacuum-dried for 6 h at 30 °C, and kept at 4 °C until further experiments.

b. Thermal grafting. The PCL films were functionalized with polyNaSS using a grafting "from" technique. 6 PCL films (14-mm diameter) were placed in 100 ml of distilled water and ozonated for 20 min at 30 °C under stirring. Ozone was generated using an ozone generator BMT 802N (ACW) with a gas pressure of 0.5 bars and an oxygen flow rate of $0.6\,l\,min^{-1}$. Next, the ozonated PCL samples were transferred in a degassed aqueous NaSS solution (15%, w/v) under argon and maintained for 1 h at 45 °C under stirring to allow for radical polymerization of the monomer. The samples were then extensively washed with distilled water for 48 h and then vacuum-dried.

3. Preparation of the samples for cell culture

Prior to the experiments, all PCL films were packaged and sterilized as follows: 2× washing (3 h in 1.5M NaCl), 1× washing (10 min in ultrapure water), 2× washing (3 h in 0.15M NaCl), 1× washing (10 min in ultrapure water), 1× washing [3 h in DPBS (Gibco, Carlsbad, USA)], 20 min in 70% ethanol, 10 min in ultrapure water, and 15 min UV irradiation (both sides of the samples). All washing steps were performed under stirring. The PCL films were kept in sterile phosphate-buffered saline (PBS) solution at −20 °C until further experiments. The samples were then slowly thawed and placed overnight at 37 °C under 5% CO_2 in DMEM (Gibco) without supplementation followed by an overnight incubation at 37 °C under 5% CO_2 in DMEM supplemented with 10% FBS except for the adhesion tests where supplementation with different protein solutions was used.

B. Chemical characterization

1. Determination of molecular weights

The PCL number average molecular weight (Mn), weight average molecular weight (Mw), and polydispersity index (PDI) were determined by size exclusion chromatography analysis using a Shimadzu Prominence instrument LC20AD pump equipped with a SIL-20ACHT auto sampler and a Shimadzu RID-10A differential refractive index detector (Shimadzu Europa GmbH, Duisburg, Germany). The samples were dissolved in tetrahydrofuran (ROTISOLV CLHP, Roth Sochiel EURL, Lauterbourg, France) at

5 mg ml^{-1} and eluted through two columns (phenomenex phenogel, Torrance, USA). A conventional calibration curve was generated using a series of narrow polydispersity poly(-methyl methacrylate) standards. Three samples were analyzed per condition.

2. Differential scanning calorimetry method

Differential scanning calorimetry (DSC) analyses were carried out with a DSC 8000 calorimeter (Perkin Elmer, Waltham, USA) under the nitrogen atmosphere. The samples were scanned once from −80 to 100 °C at a heating rate of 10 °C min^{-1}. The glass transition temperature (T_g), melting temperature (T_m), and melting enthalpy (ΔH_m) of the PCL films were determined from this first scan. The glass transition temperature was assessed using the midpoint method (temperature at which the measured curve is equidistant between the upper and lower tangents). The melting temperature was taken at the maximum of the melting peak. The melting enthalpy was calculated as the area under the melting peak. The degree of crystallinity (X_c) was calculated according to Eq. (1),[30]

$$X_c = \Delta H_m/\Delta H_{m0} \times 100, \quad (1)$$

where ΔH_{m0} stands for the melting enthalpy of 100% crystalline PCL ($\Delta H_{m0} = 135.44$ J g^{-1}).[31,32]

3. Atomic force microscope

Atomic force microscope (AFM) images of the PCL films surface were acquired on air in the ScanAsyst mode using a MultiMode 8 AFM microscope (Bruker, Billerica, USA) and the NANOSCOPE ANALYSIS 1.8 software (Bruker). The regions of interest for scanning were selected using the built-in optical microscope of the AFM instrument.

4. Colorimetric method

The evidence for pNaSS grafting was tested using the toluidine blue colorimetric assay. The method described by Ciobanu *et al.*[33] was adapted as follows: an aqueous solution of toluidine blue (Roth Sochiel EURL) was prepared at 5×10^{-4}M and drops of 1M NaOH were slowly added to reach and maintain the *p*H solution value of 10.0 ± 0.1. Samples were immersed in 5 ml of this solution at 30 °C for 6 h. The stain complexed with the anionic groups of the pNaSS grafted from the surface of the films. After incubation, the samples were removed and washed three times in 5 ml of 10^{-3}M NaOH for 5 min to remove noncomplexed molecules. Each film was then placed in 10 ml of aqueous acetic acid solution (50%, v/v) for 24 h at room temperature to obtain the complete decomplexation of toluidine blue. The decomplexation solution was analyzed by UV/visible spectroscopy (Perkin Elmer lambda 25 spectrometer, Waltham, USA) at 633 nm. On the grafted surfaces, 1 mol of toluidine blue was assumed to complex 1 mol of the sulfonate group of pNaSS. The grafting rate (GR) was then calculated according to Eq. (2),

$$GR\ (mol/g) = (OD*V)/(e*l*m), \quad (2)$$

where OD is the optical density, V is the aqueous acetic acid volume (l), ϵ is the extinction coefficient of toluidine blue solution (l mol^{-1} cm^{-1}), l is the length of the spectrophotometer tank (cm), and m is the mass of the PCL films (g). The extinction coefficient was calculated based on a dilution curve using the initial toluidine blue solution.

5. X-ray photoelectron spectrometry (XPS) analysis

All spectra were taken on a Surface Science Instruments S-probe spectrometer that has a monochromatized Al Kα x rays and a low energy electron flood gun for charge neutralization of nonconducting samples. The samples were attached to the sample holder using double-sided tape and run as insulators. X-ray spot size for these acquisitions was approximately 800 μm. Pressure in the analytical chamber during spectral acquisition was less than 5×10^{-9} Torr. Pass energy for survey spectra (to calculate composition) was 150 eV, and pass energy for high-resolution scans was 50 eV. The take-off angle (angle between the sample normal and the input axis of the energy analyzer) was approximatively 0°. This take-off angle corresponds to a sampling depth of approximately 100 Å. The SERVICE PHYSICS HAWK DATA ANALYSIS software was used to determine peak areas, to calculate the elemental compositions from peak areas above a linear background, and to peak fit the high-resolution spectra. The binding energy scales of the high-resolution spectra were calibrated by assigning the lowest binding energy C1s high-resolution peak a binding energy of 285.0 eV. Three spots were analyzed on each sample. Analysis included a survey spectrum, detail spectra of Na, S, and Si, and a high-resolution spectrum of the C1s peak from one spot of each sample.

C. Cell culture analyses

1. Isolation and culture of primary sheep anterior cruciate ligament fibroblasts

Anterior cruciate ligaments (ACLs) were isolated from one sheep (2-year old female Merino sheep free of degenerative joint disease, ~60 kg) in accordance with the German legislation on protection of animals and the NIH Guidelines for the Care and Use of Laboratory Animals (NIH Publication 85–23, Rev. 1985), and was approved by the local governmental animal care committee.[34] Tissues were cut into small pieces 1–2 mm^2, washed three times in DPBS, and incubated in a 0.1% (w/v) collagenase (Sigma-Aldrich) for 6 h at 37 °C under 5% CO_2. This solution was then centrifuged 3 min at 1500 rpm and the clot resuspended in DMEM complemented with 10% bovine calf serum (Sigma-Aldrich), 1% penicillin-streptomycin (Gibco), and 1% L-glutamine (Gibco). The primary sheep ACL (sACL) fibroblasts were maintained in T-75 flasks until confluence

was reached. pNaSS-grafted and ungrafted PCL films were placed on the bottom of a 24-well plate using Teflon inserts. The cells were then seeded at a density of 5×10^4 cells/well and cultured at 37 °C under 5% CO_2 over the time of experiment.

2. Cell viability

sACL fibroblasts were maintained on PCL films for 24 h in DMEM complemented with 10% serum. The medium was removed and the samples carefully placed in new wells, washed once with PBS and 500 μl of MTT solution (Sigma, Saint Louis, USA) at a final concentration of 1 mg ml^{-1} diluted in fresh culture medium without phenol red was added. The seeded samples were incubated for 4 h at 37 °C in MTT solution. The supernatant was then discarded, and 350 μl of dimethyl sulfoxide was added to each well for 10 min at room temperature. Each well was thoroughly mixed, and the absorbance was read at 570 nm. The percentage of live cells in the presence of the PCL films was calculated using a calibration curve between the number of cells and the corresponding absorbance.

3. Cell proliferation

sACL fibroblasts were maintained on PCL films for 1, 3, or 7 days in DMEM complemented with 10% serum. The medium was then removed and the samples carefully placed in new wells, washed twice with PBS, and a solution of 0.05% trypsin-ethylenediamine tetra-acetic acid (EDTA) (Gibco) was added for 10 min at 37 °C. DMEM supplemented with serum was added and thoroughly mixed in each well for cell harvesting and counting using a Scepter 2.0 Cell Counter (Merck-Millipore, Billerica, USA). The cell doubling time was calculated according to the formula [Eq. (3)],[35]

$$DT = (T - T_0)Ln(2)/(Ln(N) - Ln(N_0)), \quad (3)$$

where $T - T_0$ is the duration of culture in hours between the initial seeded time T_0 and the observation time T, N_0 is the number of cells at time T_0, and N is the number of cells at time T.

4. Histological and fluorescence analyses

sACL fibroblasts were harvested, fixed for 30 min with 4% formaldehyde, and rinsed twice with PBS. For histological analyses (hematoxylin and eosin—H&E—staining), hematoxylin (Carl Roth GmbH, Karlsruhe, Germany) was first added to each well for 10 min. The wells were then washed once with distilled water, and a solution of 1% HCl was briefly added. Prewarmed water (60 °C) was added for 4 min, followed by addition of hematoxylin for 3 min, removal, and washing once with distilled water. The cells were then incubated with eosin (Carl Roth GmbH) for 2 min and extensively washed with distilled water. Stained samples were kept at 4 °C until observation under a light microscope (Olympus BX 45, Hamburg, Germany). For fluorescence analyses, the cells were fixed and the samples washed once with PBS and once with 3% bovine serum albumin (BSA)/PBS (Acros Organics, Geel, Belgium). The cells were then permeabilized with 0.1% Triton-X 100 in PBS for 5 min at room temperature. After two washes in PBS, the samples were incubated in 3% BSA/PBS for 1 h at room temperature. The cells were then incubated with Fluorescein Phalloidin (FITC, Molecular probes, Eugene, USA) at 1:40 in 1% BSA/PBS for 1 h at room temperature in the dark. After two washes in PBS, 2% 4′,6-diamidino-2-phenylindole (DAPI) dissolved in distilled water was added for 10 min at room temperature. The samples were stored in distilled water at 4 °C until observation under a fluorescent microscope (Olympus CKX41).

5. Immunoassay

Production of the basic fibroblast growth factor (FGF-2) and TGF-β was monitored by specific ELISAs (FGF-2 Quantikine ELISA—DFB50—and TGF-β Quantikine ELISA—DB100B, both from R&D Systems, Wiesbaden, Germany) according to the manufacturer's protocols. Cell culture supernatants were collected at the denoted time points 24 h after changing to conditioned medium. Absorbances were measured with a GENios spectrophotometer (Tecan, Crailsheim, Germany).

6. Total RNA extraction and real-time RT-PCR analyses

Cells were detached using trypsin-EDTA at 0.05% (Gibco) and collected via centrifugation for 8 min at 5000 rpm. Total cellular RNA was extracted using the RNeasy Mini Kit with an on-column RNase-free DNase treatment (Qiagen, Hilden, Germany). Reverse transcription was carried out using the 1st Strand cDNA Synthesis kit for RT-PCR (Roche Applied Science, Mannheim, Germany), and cDNA products were amplified by real-time PCR on an Mx3000P QPCR operator (Stratagene Agilent Technologies, Waldfronn, Germany) with the Brilliant SYBR Green QPCR Master Mix (Stratagene Agilent Technologies) using the following conditions: denaturation (95 °C, 10 min), amplification by 70 cycles (denaturation at 95 °C, 30 s; annealing at 55 °C, 1 min; extension at 72 °C, 30 s), denaturation (95 °C, 1 min), and final incubation (55 °C, 30 s). The primers (Invitrogen GmbH, ThermoFisher Scientific, Karlsruhe, Germany) used were type-I collagen (ligament marker) (forward 5′-ACGTCCTGGTGAAG TTGGTC-3′; reverse 5′-ACCAGGGAAGCCTCTCTCTC-3′), type-III collagen (ligament marker) (forward 5′-CACAAGGAGTCTGCATGTCT-3′; reverse 5′-GTTCACCAGGCTCACCAGCA-3′), and TNF-α (marker of inflammation) (forward 5′-AGAACCCCCTGG AGATAACC-3′; reverse 5′-AAGTGCAGCAGGCAGAAG AG-3′), and glyceraldehyde-3-phosphate dehydrogenase (GAPDH) (housekeeping gene and internal control) (forward 5′-GAAGGTGAAGGTCGGAGTC-3′; reverse 5′-GAAGAT GGTGATGGGATTTC-3′) (all 150 nM final concentration). The threshold cycle (Ct) value for each gene of interest was

measured for each amplified sample by using the MXPRO QPCR software (Stratagene Agilent Technologies) and values were normalized to GAPDH expression by using the $2^{-\Delta\Delta Ct}$ method.

7. Adhesion assay

PC12 samples were incubated at 37 °C during 2 h in DMEM complemented with 10% FBS, Fn (20 μg ml^{-1}), collagen (7 μg ml^{-1}), plasma (10%), or fibrinogen (0.3 g l^{-1}). 5×10^4 sACL fibroblasts were then seeded on the proteins preadsorbed PCL films and incubated for 15 min, 30 min, 1 h, 2 h, or 4 h at 37 °C under 5% CO_2. The supernatants were collected and the nonadhesive cells (N1) were counted using a Scepter 2.0 Cell Counter (Merck-Millipore). The samples with adhesive cells were centrifugated for 15 min at 140, 280, or 360 rpm (6, 17.5, or 25.5 dynes/cm^2, respectively). Cells removed by the applied force (N2) were counted, and the remaining adhesive cells (N3) were collected by incubation with 0.05% trypsin-EDTA (Gibco) for 10 min at 37 °C and counted. The percentages of adhesive cells under static and dynamic conditions were determined as follows [Eqs. (4) and (5)—adapted from Felgueiras *et al.*[36]]:

$$\%_{\text{static adhesive cells}} = \frac{N2 + N3}{N1 + N2 + N3} \times 100, \quad (4)$$

$$\%_{\text{dynamic adhesive cells}} = \frac{N3}{N2 + N3} \times 100. \quad (5)$$

D. Statistical analysis and software

All the experiments were carried out a minimum of three times except for the morphology study which was performed using one sample per condition and for the adhesion assay with several proteins which was done using two samples per condition. Statistical analyses were performed with EXCEL software using ANOVA and $p \leq 0.05$ was considered statistically significant. The cell densities were measured with the IMAGE J software (Wayne Rasband, Bethesda, USA) based on at least three different images.

III. RESULTS

A. Chemical characterization

1. Comparison of PC12 and PC60 films

The PC60 films had an Mn value of 60 614 ± 743 g mol^{-1} and a PDI of 1.29 ± 0.01, while the PC12 films had an Mn value of 80 481 ± 1554 g mol^{-1} and a PDI of 1.26 ± 0.02 (Table I). Neither the T_g (approximately −60°C) nor the T_f (approximately +60°) were significantly different between the two types of films and were consistent with values found in the literature (Table II). The percentage of crystallinity (~64%) was also similar for both films (Table II). The observed microstructure of the films was consistent with these DSC analyses. The shape of the spherulites identified by AFM did not vary [Figs. 1(a) and 1(b)]. Despite the different average chain lengths of the two films, both PCL films had a PDI close to 1.

TABLE I. Molecular weights of the films (NG: nongrafted films; G: grafted films; Mn: number average molecular weight; Mw: weight average molecular weight; PDI: polydispersity index).

Films	Mn (kg/mol)	Mw (kg/mol)	PDI
PC60 (NG)	60.6 ± 0.7	78.0 ± 0.8	1.29 ± 0.01
PC60 (G)	60.3 ± 1.0	77.5 ± 1.0	1.29 ± 0.01
PC12 (NG)	80.5 ± 1.6	97.7 ± 0.5	1.26 ± 0.02
PC12 (G)	77.2 ± 1.1	98.9 ± 0.2	1.28 ± 0.01

2. Characteristics of pNaSS grafting

The presence of pNaSS molecules grafted on the films was assessed by a colorimetric method (toluidine blue assay) and XPS analysis. The toluidine blue assay gave a GR of 10.5 ± 0.1 μmol g^{-1} for the PC60 films and of 6.8 ± 1.9 μmol g^{-1} for the PC12 films (Table III). Negative controls (natural fixation of toluidine blue molecules to the polymer itself) were performed using both types of nongrafted films. The values obtained from the grafted samples were negligible compared with the grafted samples. XPS analysis only detected the presence of sulfur and Na atoms on the grafted films (Table III). The GR values obtained by sensitive toluidine blue assay correlated well with the percentages of sulfur atoms measured by XPS. In both types of films, the presence of sulfur atoms was linked to a decrease in carbon concentration and to an increase in oxygen concentration (Fig. 2). This observation confirmed the mechanism of grafting presented by Ciobanu *et al.*[33] and Rohman *et al.*,[37] which started with an oxidation of the surface to generate peroxide and hydroperoxide functions followed by radical polymerization of NaSS.

3. Impact of pNaSS grafting on the PCL structure

The radical grafting of pNaSS did not modify the Mn value of the PC60 films nor their PDI (Table I). Nevertheless, the thermal analysis revealed a slight increase in T_g from −61.5 ± 0.5 °C to −59.7 ± 0.6 °C and a slight increase in T_f from 60.1 ± 0.5 °C to 60.9 ± 0.1 °C (Table II). The decrease in percentage of crystallinity from 64.1 ± 6.5% to 61.8 ± 8.3% was not significant ($p > 0.05$), consistent with

TABLE II. DSC analysis of the films (NG: nongrafted films; G: grafted films).

Films	T_g (°C)	T_f (°C)	ΔH (J/g)	χ (%)
PC60 (NG)	−61.5 ± 0.5	60.1 ± 0.5	86.9 ± 8.9	64.1 ± 6.5
PC60 (G)	−59.7 ± 0.6	60.9 ± 0.1	83.8 ± 11.2	61.8 ± 8.3
PC12 (NG)	−60.9 ± 0.1	60.8 ± 0.1	87.7 ± 4.2	64.7 ± 3.3
PC12 (G)	−62.2 ± 0.5	61.2 ± 0.1	83.6 ± 4.4	61.7 ± 3.3

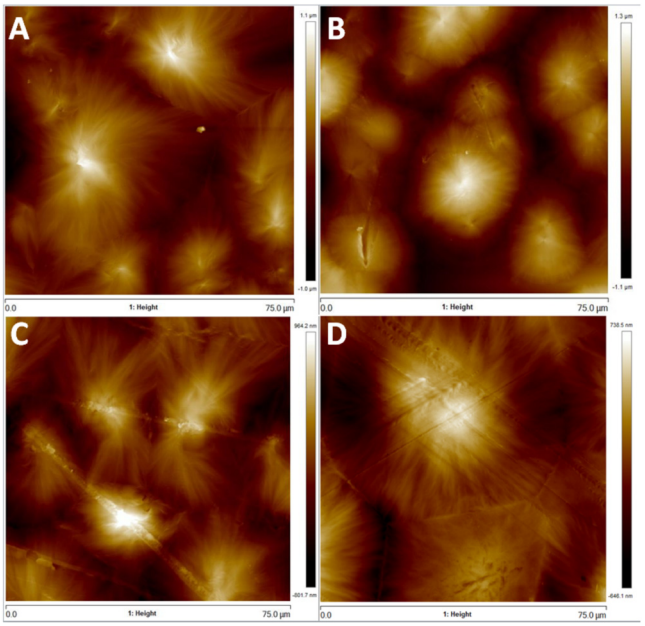

FIG. 1. AFM images of (a) a nongrafted PC60 film, (b) a nongrafted PC12 film, (c) a grafted PC60 film, and (d) a grafted PC12 film.

the AFM images of the PC60 films [Figs. 1(a) and 1(c)], confirming the absence of detectable modification of the microstructure. On the PC12 films, grafting led to a significant decrease of the Mn value (from 80.5 ± 1.6 to $77.2 \pm 1.1\ \mathrm{kg\,mol^{-1}}$) ($-4.05\%$, $p \leq 0.05$) (Table I). This decrease in length of the molecular chains was consistent with the observed decrease in T_g from $-60.9 \pm 0.1\ ^\circ\mathrm{C}$ to $-62.2 \pm 0.5\ ^\circ\mathrm{C}$ (Table II). The slight increase in T_f from $60.8 \pm 0.1\ ^\circ\mathrm{C}$ to $61.2 \pm 0.1\ ^\circ\mathrm{C}$ was consistent with the observation of the AFM images of the PC12 films [Figs. 1(b) and 1(d)] that revealed an important augmentation of the spherulite size after grafting. Although the percentage of crystallinity decreased from $64.7 \pm 3.3\%$ to $61.7 \pm 3.3\%$, this change was not significant ($p > 0.05$). The PC12 films appear to be more sensitive to the grafting process compared to the PC60 films.

B. Impact on biologic behavior

1. Cell viability

The percentages of live sACL fibroblasts seeded on the films were of $107.3 \pm 7.2\%$ for the PC60 films and of $97.2 \pm 0.3\%$ for the PC12 films compared with the $100.0 \pm 0.2\%$ control without any films, revealing the lack of cytotoxicity of the PCL films, regardless of their molecular weight (Fig. 3). When seeded on the grafted materials, the levels of cell viability were still high (>97% live cells). PCL is a well-known biocompatible polymer already used in many medical devices including sutures, dressings, and contraceptive devices.[11] The observed results confirmed the absence of cytotoxicity for both PCL and pNaSS-grafted PCL films when placed in direct contact with primary sACL fibroblasts as a model to study ACL reconstruction.

2. Cell proliferation

Evaluation of the sACL fibroblast numbers over time in the absence of films (positive control) revealed low levels of cell proliferation, with a cell doubling time of 5.2 ± 0.1 days [Fig. 4(b)]. The results obtained with the PCL films showed that the number of cells was lower compared to the positive control at all time points evaluated [Fig. 4(a)]. An estimation of the cell doubling time revealed no significant difference between the PC12 cultures and the positive control (6.4 ± 0.8 vs 5.2 ± 0.1 days) while a significant increase was noted for the PC60 cultures relative to the positive control (9.6 ± 1.4 vs 5.2 ± 0.1 days) [Fig. 4(b)]. The presence or the absence of pNaSS grafting on the PC12 films did not significantly impact the rate of proliferation whereas grafting on the PC60 films improved the rates of cell growth (8.5 ± 0.2 days for grafted PC60 films vs 10.8 ± 0.6 days for nongrafted PC60 films).

3. Cell characterization

Labeling of sACL fibroblasts maintained with PC60 films (Fig. 5) showed that surface modification with pNaSS-grafted films [Figs. 5(d)–5(f)] promoted the development of a higher cytoskeleton network in the cells compared to non-grafted films [Figs. 5(a)–5(c)]. This enhancement could be observed after 1 day. and it progressively increased over time until after 7 days the actin network was well developed and oriented in a longitudinal axis [Fig. 5(f)]. An analysis by H&E staining further revealed that while no significant differences in the cell attachment patterns were seen early on between grafted and nongrafted films [insets of Figs. 5(a), 5(b), 5(d), and 5(e)], a more homogeneous distribution of the cells was noted in the presence of the grafted films on day 7 [insets of Fig. 5(f) versus Fig. 5(c)]. The cells were also more homogeneously distributed on the grafted films

TABLE III. Grafting rates (NG: nongrafted films; G: grafted films; GR: grafting rate; XPS: x-ray photoelectron analysis).

		XPS atomic concentration (%)					
Films	GR (μmol/g)	C 1s	O 1s	S 2p	Na 1s	Si 2p	Others
PC60 (NG)	0.7 ± 0.3	72.1 ± 0.9	22.7 ± 0.9	—	—	3.4 ± 0.1	trace N 1s. F 1 s. Sn 3d5
PC60 (G)	10.5 ± 0.1	61.4 ± 0.7	29.6 ± 0.8	1.8 ± 0.1	0.9 ± 0.1	1.5 ± 0.4	trace Mg 2s. Sn 3d5
PC12 (NG)	0.9 ± 0.3	74.4 ± 0.7	24.2 ± 0.3	—	—	1.1 ± 0.3	trace F 1s
PC12 (G)	6.8 ± 1.9	56.2 ± 1.2	31.7 ± 0.3	1.6 ± 0.1	0.7 ± 0.1	2.1 ± 0.1	trace Al 2s. Mg 2s

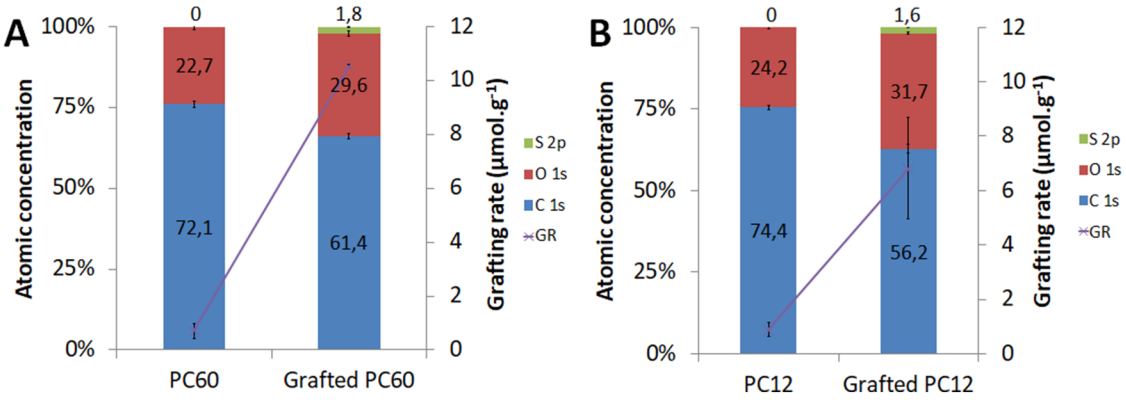

FIG. 2. Evolution of the XPS atomic concentration percentages for the (a) PC60 and (b) PC12 films (GR: grafting rate).

compared with the nongrafted films [insets of Figs. 5(d)–5(f) versus Figs. 5(a)–5(c), respectively]. Of further note, the morphology of the cells was more fusiform in the presence of the grafted films and their color showed a good vitality in these cultures. These findings were corroborated by the estimated cell densities, showing a significant increase (1.7-fold, $p \leq 0.05$) in the grafted films (~59 600 cells/cm^2) compared to the nongrafted films (~34 700 cells/cm^2) at day 7 [Fig. 5(i)].

Similar observations were noted when growing sACL fibroblasts on PC12 films over time (Fig. 6), with a more developed skeleton network [Fig. 6(f) versus Fig. 6(c)], a more homogeneous cell distribution [insets of Fig. 6(f) versus Fig. 6(c)], higher vitality, and significantly higher cell densities after 7 days when using grafted films (e.g., ~24 000 cells/cm on nongrafted films vs ~65 700 cells/cm^2 on grafted films) [Fig. 6(i)]. Interestingly, the increase in cell density upon grafting was higher for the PC12 films compared to the PC60 films [2.7 versus 1.7 fold increases, see Fig. 5(i) and 6(i)].

C. Growth factor production

The production of FGF-2 and TGF-β was measured over time in sACL fibroblasts seeded on the various films

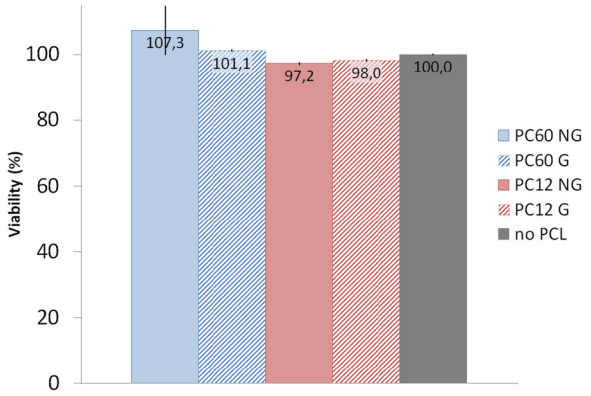

FIG. 3. Viability of sACL fibroblasts in the presence of the PCL films. An MTT assay was performed after 24 h of contact between the cells and the various films as described in Sec. II (NG: nongrafted films; G: grafted films).

(Fig. 7). In the absence of films, the cells significantly secreted 3- to 20-fold more TGF-β [Figs. 7(c) and 7(d)] than FGF-2 [Figs. 7(a) and 7(b)] ($p \leq 0.005$), showing however a 1.2-fold decrease in TGF-β expression between days 5 and 7 ($p \leq 0.005$) and an average of 2.9-fold decrease in FGF-2 expression over time ($p \leq 0.005$). Interestingly, the production of the two growth factors was significantly stimulated upon seeding of the cells on the films, regardless of types of films. On day 5, an increase in FGF-2 production (1.9- and 1.5-fold) and in TGF-β production (4.8- and 2.1-fold) was noted versus controls for the PC60 and PC12 films, respectively ($p \leq 0.05$). After 7 days, the levels of FGF-2 were 1.6-fold ($p > 0.05$) and 1.7-fold ($p \leq 0.05$) higher than the controls for the PC60 and PC12 films, respectively, while those of TGF-β were 4.8- and 1.6-fold higher ($p \leq 0.05$). Such stimulating effects were well pronounced after 5 days and maintained on day 7. Of note, the presence of pNaSS grafting did not impact release of the growth factors ($p > 0.005$).

D. Gene expression

The gene expression profiles of type-I and -III collagen (ligament markers) as well as those of TNF-α (inflammatory marker) were monitored in sACL fibroblasts over culture time for the different films (Fig. 8). When cells were grown on PC60 films [Figs. 8(a)–8(c)], the levels of expression of the different genes were always higher on day 7 compared with day 5. Type-I collagen expression was more elevated after 7 days in the presence of films relative to the control (no film) (3.1- and 1.7-fold for nongrafted and grafted PC60 films, respectively, $p > 0.05$) [Fig. 8(a)]. In contrast, type-III collagen expression was always below the levels of the control (day 5: 9.3- and 27.7-fold lower for nongrafted and grafted PC60 films, respectively, $p \leq 0.005$; day 7: 1.4-fold and 1.1-fold lower for nongrafted and grafted PC60 films, respectively, $p > 0.05$) [Fig. 8(b)]. The only significant difference observed for TNF-α expression levels between the film versus control was at day 5 for the nongrafted PCL film [0.4-fold difference, $p \leq 0.05$, see Fig. 8(c)]. In general, there was no significant difference between grafted and nongrafted PC60 samples for any of the genes analyzed

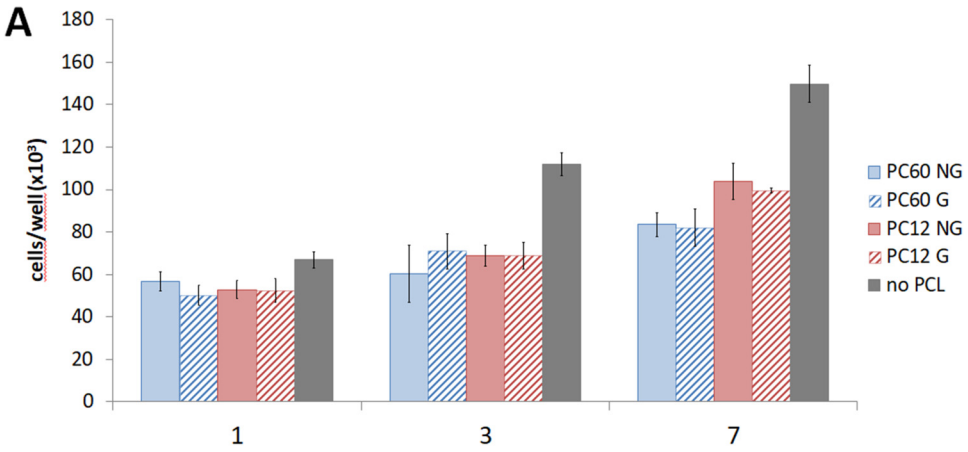

B

PC60		PC12		no PCL
NG	G	NG	G	
10.8 ± 0.6	8.5 ± 0.2	6.2 ± 0.1	6.6 ± 1.4	5.2 ± 0.02
9.6 ± 1.4		6.4 ± 0.8		

FIG. 4. Proliferation of sACL fibroblasts over time in the presence of the PCL films. The numbers of adherent cells (a) and the cell doubling time (days) (b) were measured at the time points (NG: nongrafted films; G: grafted films).

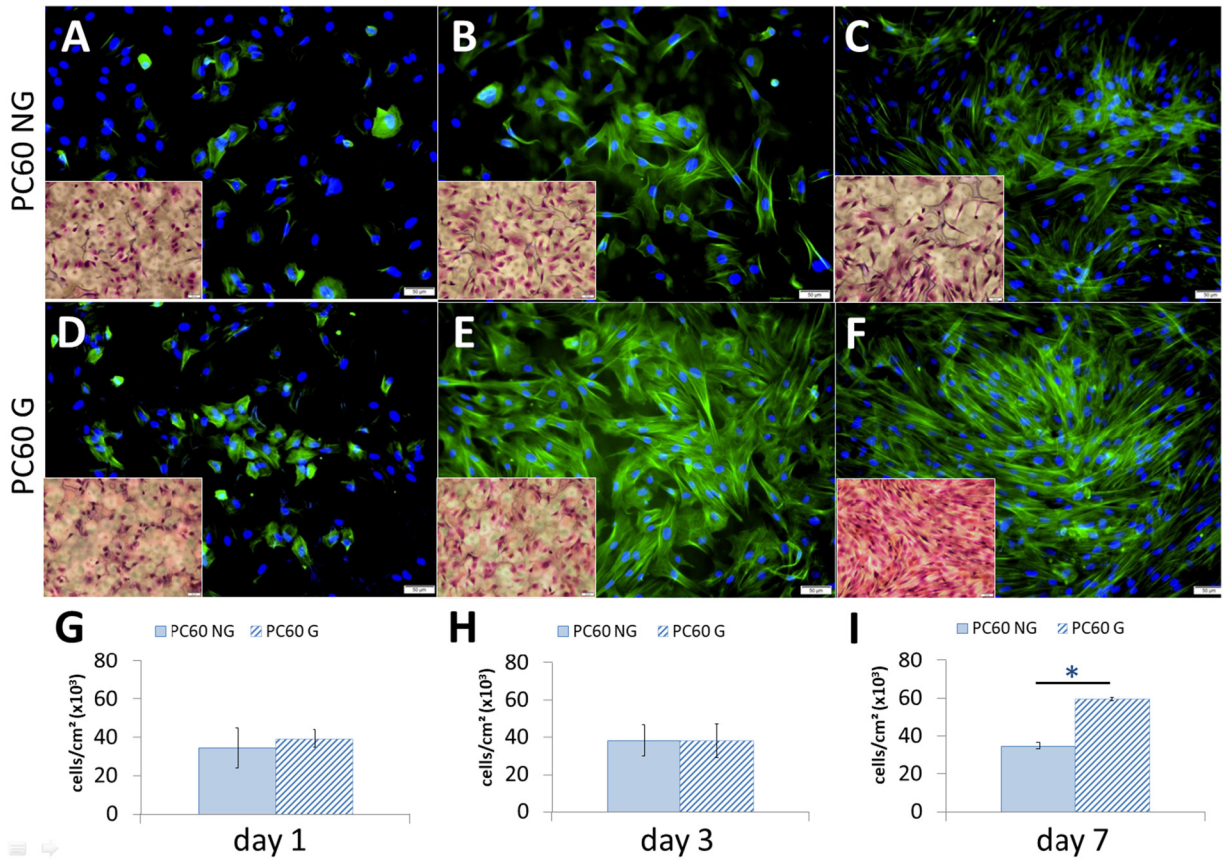

FIG. 5. Characterization of sACL fibroblasts over time in the presence of the PCL films (PC60). Phalloidin (green)/DAPI (blue) labeling and H&E staining (insets) and corresponding cell densities (cell/cm^2) [(g)–(i)] were performed at day 1: [(a), (d), and (g)]; day 3: [(b), (e), and (h)]; day 7: [(c), (f), and (i)]. NG: nongrafted films; G: grafted films. *Statistically significant relative to the corresponding NG condition.

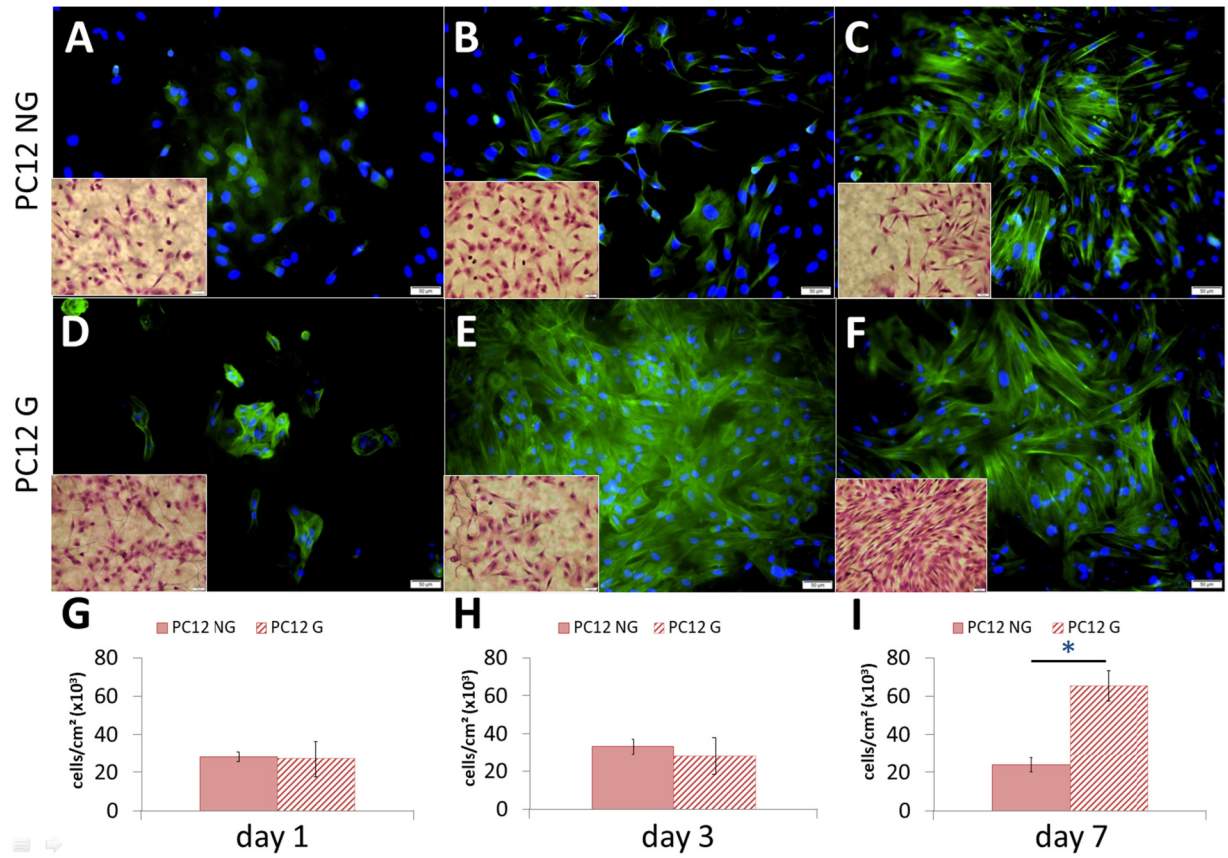

FIG. 6. Characterization of sACL fibroblasts over time in the presence of the PCL films (PC12). Phalloidin (green)/DAPI (blue) and H&E staining (insets) with corresponding cell densities (cell/cm^2) [(g)–(i)] were performed at day 1: [(a), (d), and (g)]; day 3: [(b), (e), and (h)]; day 7: [(c), (f), and (i)]. NG: nongrafted films; G: grafted films.

($p > 0.005$). When cells were grown on grafted PC12 films [Figs. 8(d)–8(e)], the type-I collagen expression was similar to the control (no film), while the levels were significantly lower than the control with the non grafted film at day 5 [Fig. 8(d)]. The levels for type-III collagen expression were always lower than the control [Fig. 8(e)]. The TNF-α expression levels were significantly lower for both the grafted and nongrafted films versus the control at day 7 (4.2- and 6.7-fold difference, $p \leq 0.05$) [Fig. 8(f)].

1. Kinetics of cell adhesion on PC12 films

Adhesion assays were only performed with the PC12 films as this material was capable of both supporting the early formation of a collagen matrix and containing potential inflammatory responses. The initial adhesion strength of sACL fibroblasts seeded on PC12 films was evaluated after preincubation of the surfaces with DMEM supplemented with 10% FBS. The static cell adhesion over time had similar curve shapes for the grafted and nongrafted films, but with fewer cells adhered on the nongrafted films [Fig. 9(a)]. The higher cell adhesion onto the grafted films becomes significant after 30 min of incubation. Therefore, this time of cell incubation was chosen for the centrifugal force experiments [Fig. 9(b)]. τ_{50} was determined as the shear stress corresponding to the strength where 50% of the cells detached. The τ_{50} was ~17.5 and ~25.5 dynes/cm^2 for cells seeded on nongrafted films and grafted films, respectively. Thus, the cell adhesion strength increased as a result of pNaSS grafting. When the effect was studied over time, cells needed to be incubated for 4 h for the nongrafted and grafted films to have similar adhesion strengths [Fig. 9(c)].

2. Adhesion mechanisms in the presence of pNaSS grafting

Static and dynamic adhesions of sACL fibroblasts seeded 30 min on PC12 films with preadsorbed proteins were studied. Because DMEM supplemented with 10% FBS contains proteins at a concentration that is 10-fold lower than normal human serum, Fn, collagen, or fibrinogen alone in medium and 10% plasma-DMEM were studied. After 30 min cell incubation, the percentage of static adherent cells was not different on the grafted versus nongrafted films in the presence of preadsorbed Fn, preadsorbed collagen or DMEM with 10% FBS. On the other hand, a trend toward an increase in adherent cells on the grafted films under static conditions was noted with medium containing 10% plasma and this difference became significant when fibrinogen was used alone [Fig. 10(a)]. These observations were confirmed with the dynamic adhesion assay [Fig. 10(b)]. Indeed, the

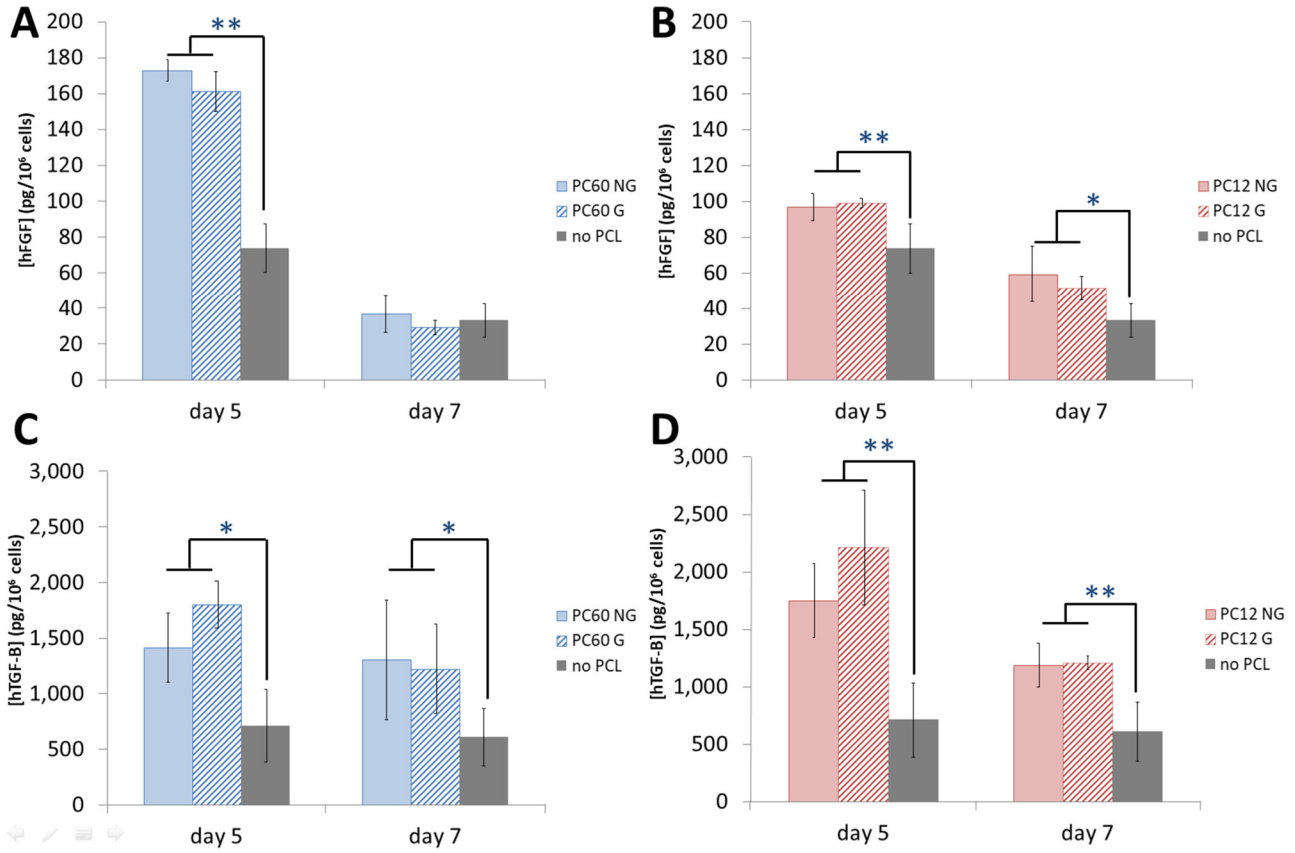

FIG. 7. Production of FGF-2 [(a) and (b)] and TGF-β [(c) and (d)] from sACL fibroblasts over time in the presence of the PCL films [PC60 films: (a) and (c); PC12 films: (b) and (d)]. Growth factor expression was measured by ELISA. NG: nongrafted films; G: grafted films (*$p \leq 0.05$ and ** $p \leq 0.005$).

presence of Fn alone adhered the cells to the surface independently of pNaSS grafting. The same phenomenon was observed to a lesser extent with collagen alone. In contrast, pNaSS grafting highly interacted with the cells in the presence of preadsorbed plasma or fibrinogen, increasing their adhesive strength.

VI. DISCUSSION

The development of a biomaterial, especially a biodegradable one, can be challenging in terms of chemistry and structure.[38] Several parameters such as molecular weight, purity, or viscosity determine the ability to process the material to a specific structure,[39,40] with the processing parameters impacting the crystallinity, topography, final mechanical properties, etc. of the final product.[41,42] Also, surface properties such as ionic charge, surface energy, wettability, and/or roughness will also influence the cellular responses.[43–48]

The main differences between the two films tested in this study were the grade (technical versus medical) and the molecular weights (60 vs 80 kDa). Cui and Sinko[26] demonstrated that *in vitro*, NIH3T3 fibroblasts attach and proliferate most efficiently on a highly crystalline surface. In this study, the two different polymers had similar crystallinities, melting temperatures, and microstructures so the effect of crystallinity on cellular responses could not be investigated, but some differences between the materials were observed.

pNaSS was successfully grafted from both hydrophobic PCL films. The grafting process did not significantly modify the physicochemical properties of PC60, but it did result in a 4% decrease of the M_n and an increase in the spherulite size for the PC12 films. The biologic assays showed that both pNaSS-grafted PCL films produced a more homogeneous cell distribution, a significant higher cell density after 7 days of culture, and a more developed actin skeleton network, while pNaSS grafting only increased the cell growth rate on the PC60 films. All grafted and nongrafted PCL films produced an overproduction of FGF-2 and TGF-β relative to the control (no film) with the amount of gene expression decreasing from day 5 to day 7. Further experiments on PC12 films demonstrated that pNaSS grafting promoted early cell adhesion after 30 min of contact between the cells and materials. The early adhesion was coupled with an ~1.5-fold increase in cell adhesion strength, which was maintained over time. This phenomenon was mediated by the cell/protein/surface interactions, in particular with preadsorbed plasma proteins and fibrinogen.

It interesting to compare the results from the grafted PCL films in this study with previous studies of pNaSS grafted onto other substrates such as various forms of poly(ethylene terephthalate) (PET) and a titanium alloy

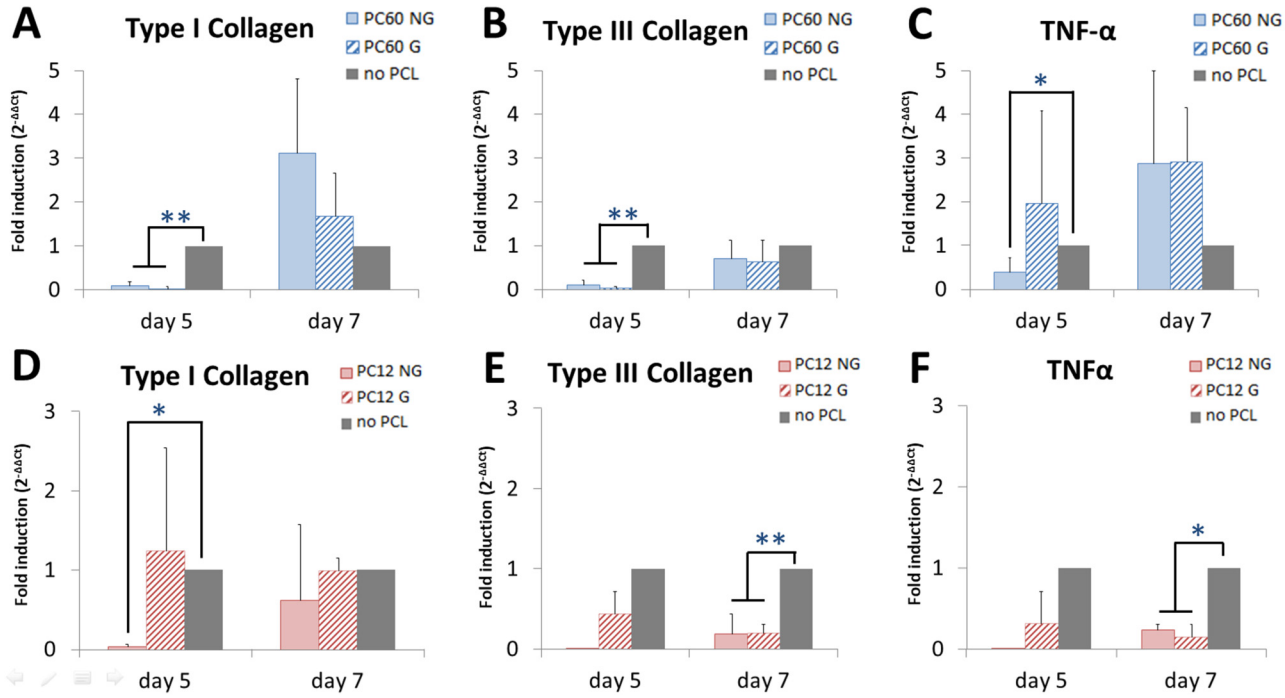

FIG. 8. Gene expression in sACL fibroblasts over time in the presence of the PCL films. Samples were processed for total cellular RNA extraction, cDNA synthesis, and real-time RT-PCR amplification. NG: nongrafted films; G: grafted films. The genes analyzed included type-I collagen [(a) and (d)], type-III collagen [(b) and (e)], and TNF-α [(c) and (f)], with GAPDH serving as a housekeeping gene and internal control. Ct values were obtained for each target and GAPDH as a control for normalization, and fold inductions (relative to cells maintained in absence of films) were measured using the $2^{-\Delta\Delta Ct}$ method (*$p \leq 0.05$ and **$p \leq 0.005$).

(TiAl6V4). Zhou *et al.*[19,49] observed a homogeneous cell distribution of human fibroblasts along pNaSS-grafted PET fibers with a more fusiform morphology that were associated with higher adhesion forces. In addition, it has been shown that the presence of pNaSS chains can induce Fn to unfold to a more stable conformation, thereby increasing the exposure of its active binding regions and therefore promoting cell attachment.[50] Felgueiras *et al.* showed the

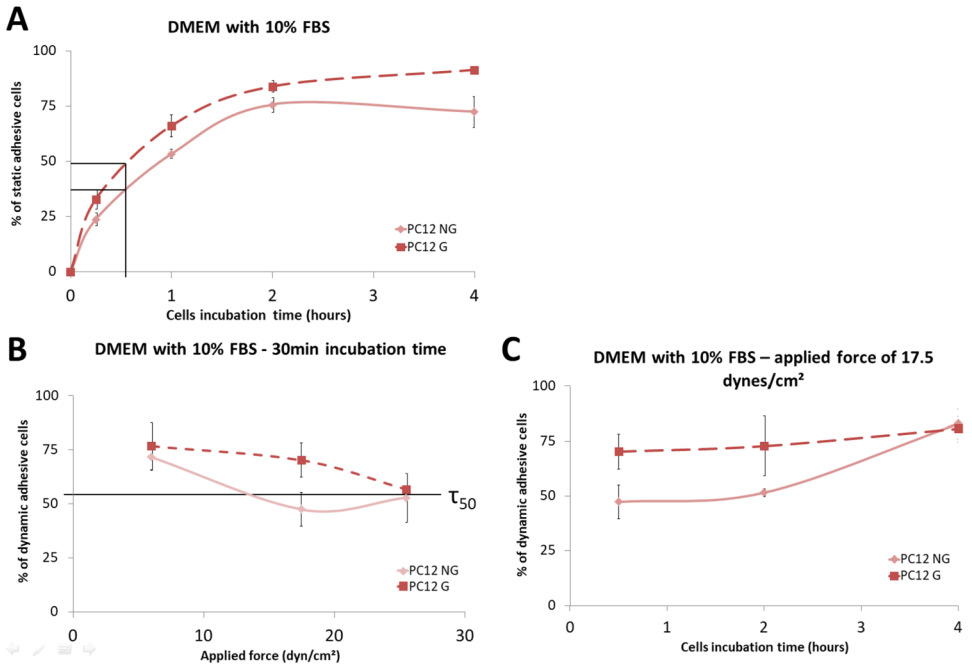

FIG. 9. Kinetics of sACL fibroblast adhesion on PC12 films preincubated with 10% FBS (NG: nongrafted films; G: grafted films). (a) Static adhesion vs cell incubation time. (b) Dynamic adhesion after 30 min of incubation and with increasing centrifugal force applied. (c) Dynamic adhesion with cell incubation time upon force application (17.5 dynes/cm^2).

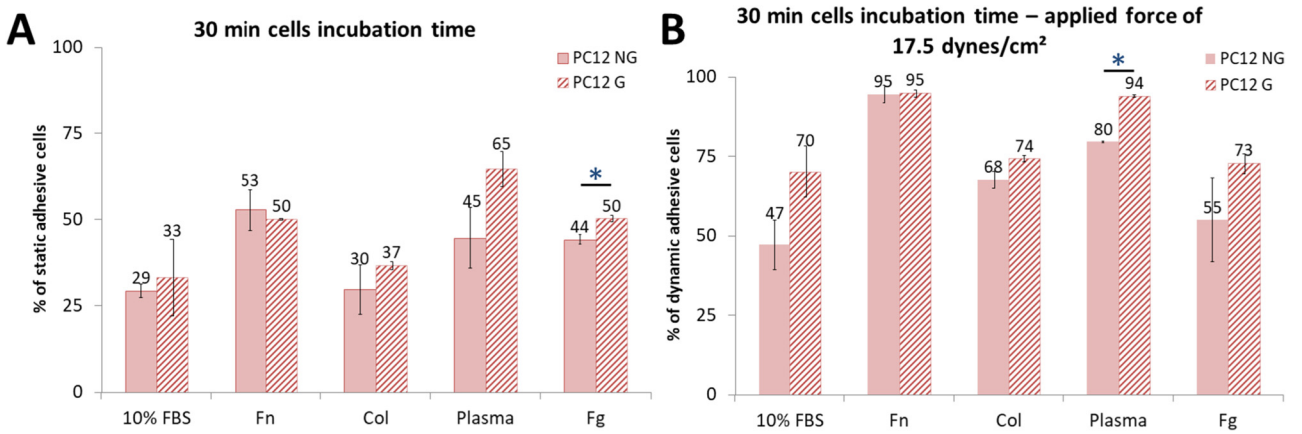

FIG. 10. Percentages of static (a) and dynamic (b) adhesion of sACL fibroblasts seeded on proteins preadsorbed PC12 films (NG: nongrafted films; G: grafted films).

presence of pNaSS modulates the Fn conformation as well as other proteins (albumin, type-I collagen, and vitronectin).[22–25] Thus, the observed effects on cell morphology and adhesion strengths are associated with the presence of pNaSS and not related to the type of substrate the pNaSS is grafted from. However, some differences in the influence of various protein preadsorbed surfaces were observed among the different pNaSS samples, which will require further investigation.

V. CONCLUSION

The goal of this study was to evaluate the early responses of sheep ACL fibroblasts on PCL films functionalized with pNaSS. The results showed no detectable impact of the pNaSS grafting process on the physicochemical properties of PC60, while some small changes were detected for pNaSS grafting from PC12. The biologic evaluations demonstrated a better cell control together with the lack of inflammation (TNF-α) when using PC12 films compared to PC60 films. Both types of films were capable of overproducing FGF-2 and TGF-β compared with the controls at early time points (day 5). These outcomes were not sufficient to enhance type-I and type-III collagen expression versus controls, which were similar by day 7. Finally, the bioactive mechanism of pNaSS grafting on PCL was observed to be consistent with previous studies on pNaSS grafting on other substrates. pNaSS grafting enhanced quick early (e.g., 30 min) cell adhesion and by day 7 resulted in increased cell density and actin network development. Overall, the use of PC12 materials coupled with pNaSS grafting show promise for applications in ligament reconstruction.

ACKNOWLEDGMENTS

This work was funded as part of the "Future Investment Project" by the French Public Investment Bank and the French state—PSPC application—Liga2bio project (VM) and by the *Deutsche Arthrose-Hilfe e.V.* (M.C.). The XPS experiments done at NESAC/Bio were supported by NIH under Grant No. EB-002027. The authors thank Gerry Hammer (NESAC/Bio) for his help with the XPS analysis.

[1]A. M. Kiapour and M. M. Murray, Bone Jt. Res. **3**, 20 (2014).
[2]A. D. Georgoulis *et al.*, Orthop. Traumatol. Surg. Res. **96**, S119 (2010).
[3]D. S. Mastrokalos, J. Springer, R. Siebold, and H. H. Paessler, Am. J. Sports Med. **33**, 85 (2005).
[4]D. E. Gwinn, J. H. Wilckens, E. R. McDevitt, G. Ross, and T.-C. Kao, Am. J. Sports Med. **28**, 98 (2000).
[5]H. H. Lu, J. A. Cooper Jr, S. Manuel, J. W. Freeman, M. A. Attawia, F. K. Ko, and C. T. Laurencin, Biomaterials **26**, 4805 (2005).
[6]G. H. Altman, R. L. Horan, H. H. Lu, J. Moreau, I. Martin, J. C. Richmond, and D. L. Kaplan, Biomaterials **23**, 4131 (2002).
[7]C. T. Laurencin and J. W. Freeman, Biomaterials **26**, 7530 (2005).
[8]J. W. Freeman, M. D. Woods, and C. T. Laurencin, J. Biomech. **40**, 2029 (2007).
[9]J. A. Cooper, J. S. Sahota, W. J. Gorum, J. Carter, S. B. Doty, and C. T. Laurencin, Proc. Natl. Acad. Sci. U.S.A. **104**, 3049 (2007).
[10]A. C. Vieira, R. M. Guedes, and A. T. Marques, J. Biomech. **42**, 2421 (2009).
[11]M. A. Woodruff and D. W. Hutmacher, Prog. Polym. Sci. **35**, 1217 (2010).
[12]H. Li *et al.*, Acta Biomater. **8**, 4007 (2012).
[13]H. Li, C. Chen, Y. Ge, and S. Chen, Biotechnol. Lett. **36**, 1079 (2014).
[14]J. Chen, G. H. Altman, V. Karageorgiou, R. Horan, A. Collette, V. Volloch, T. Colabro, and D. L. Kaplan, J. Biomed. Mater. Res. A **67**, 559 (2003).
[15]S. Font Tellado, E. R. Balmayor, and M. Van Griensven, Adv. Drug Deliv. Rev. **94**, 126 (2015).
[16]L. Stanislawski, H. Serne, M. Stanislawski, and M. Jozefowicz, J. Biomed. Mater. Res. **27**, 619 (1993).
[17]M. Jozefowicz and J. Jozefonvicz, Biomaterials **18**, 1633 (1997).
[18]F. El Khadali, G. Hélary, G. Pavon-Djavid, and V. Migonney, Biomacromolecules **3**, 51 (2002).
[19]G. Pavon-Djavid, L. J. Gamble, M. Ciobanu, V. Gueguen, D. G. Castner, and V. Migonney, Biomacromolecules **8**, 3317 (2007).
[20]S. Lessim, V. Migonney, P. Thoreux, D. Lutomski, and S. Changotade, Biomed. Mater. Eng. **4**, 289 (2013).
[21]C. Vaquette, V. Viateau, S. Guérard, F. Anagnostou, M. Manassero, D. G. Castner, and V. Migonney, Biomaterials **34**, 7048 (2013).
[22]H. Felgueiras and V. Migonney, IRBM **34**, 371 (2013).
[23]H. P. Felgueiras and V. Migonney, IRBM **37**, 165 (2016).
[24]H. P. Felgueiras, M. D. M. Evans, and V. Migonney, Acta Biomater. **28**, 225 (2015).
[25]H. P. Felgueiras, S. D. Sommerfeld, N. S. Murthy, J. Kohn, and V. Migonney, Langmuir **30**, 9477 (2014).
[26]H. Cui and P. J. Sinko, Front. Mater. Sci. **6**, 47 (2012).

[27]Z.-L. Yang, S. Zhou, L. Lu, X. Wang, J. Wang, and N. Huang, J. Biomed. Mater. Res. A **100A**, 3124 (2012).
[28]T. Marui, C. Niyibizi, H. I. Georgescu, M. Cao, K. W. Kavalkovich, R. E. Levine, and S. L-Y. Woo, J. Orthop. Res. **15**, 18 (1997).
[29]D. Amiel, C. Frank, F. Harwood, J. Fronek, and W. Akeson, J. Orthop. Res. **1**, 257 (1983).
[30]A. Heimowska, M. Morawska, and A. Bocho-Janiszewska, Pol. J. Chem. Technol. **19**, 120 (2017).
[31]H. Kweon, Biomaterials **24**, 801 (2003).
[32]L. A. Bosworth and S. Downes, Polym. Degrad. Stab. **95**, 2269 (2010).
[33]M. Ciobanu, A. Siove, V. Gueguen, L. J. Gamble, D. G. Castner, and V. Migonney, Biomacromolecules **7**, 755 (2006).
[34]L. Goebel, P. Orth, M. Cucchiarini, D. Pape, and H. Madry, Osteoarthritis Cartilage **25**, 581 (2017).
[35]A. Korzyńska and M. Zychowicz, Biocybern. Biomed. Eng. **28**, 75 (2008).
[36]H. P. Felgueiras, A. Decambron, M. Manassero, L. Tulasne, M. D. M. Evans, V. Viateau, and V. Migonney, J. Colloid Interface Sci. **491**, 44 (2017).
[37]G. Rohman, S. Huot, M. Vilas-Boas, G. Radu-Bostan, D. G. Castner, and V. Migonney, J. Mater. Sci. Mater. Med. **26**, 206 (2015).
[38]T. K. Dash and V. B. Konkimalla, J. Controlled Release **158**, 15 (2012).
[39]F. Mostafavi and N. G. Ebrahimi, J. Appl. Polym. Sci. **125**, 4091 (2012).
[40]C. G. Madsen, A. Skov, S. Baldursdottir, T. Rades, L. Jorgensen, and N. J. Medlicott, Eur. J. Pharm. Biopharm. **92**, 1 (2015).
[41]A. G. A. Coombes, S. C. Rizzi, M. Williamson, J. E. Barralet, S. Downes, and W. A. Wallace, Biomaterials **25**, 315 (2004).
[42]A. Leroux, C. Egles, and V. Migonney, PLoS ONE **13**, e0205722 (2018).
[43]D. D. Deligianni, N. Katsala, S. Ladas, D. Sotiropoulou, J. Amedee, and Y. F. Missirlis, Biomaterials **22**, 1241 (2001).
[44]K. M. Hotchkiss, G. B. Reddy, S. L. Hyzy, Z. Schwartz, B. D. Boyan, and R. Olivares-Navarrete, Acta Biomater. **31**, 425 (2016).
[45]S. Spriano *et al.*, Mater. Sci. Eng. C **74**, 542 (2017).
[46]E. Rosellini, C. Cristallini, G. D. Guerra, and N. Barbani, J. Biomater. Sci. Polym. Ed. **26**, 515 (2015).
[47]P. Shokrollahi, H. Mirzadeh, O. A. Scherman, and W. T. S. Huck, J. Biomed. Mater. Res. A **95A**, 209 (2010).
[48]J. Crispim, H. A. M. Fernandes, S. C. Fu, Y. W. Lee, P. Jonkheijm, and D. B. F. Saris, Acta Biomater. **53**, 165 (2017).
[49]J. Zhou, M. Ciobanu, G. Pavon-Djavid, V. Gueguen, and V. Migonney, "Morphology and adhesion of human fibroblast cells cultured on bioactive polymer grafted ligament prosthesis," in *2007 29th Annual International Conference of the IEEE Engineering in Medicine and Biology Society*, Lyon, France, 22–26 August (2007), pp. 5115–5118.
[50]J. D. Andrade, V. Hlady, A.-P. Wei, C.-H. Ho, A. S. Lea, S. I. Jeon, Y. S. Lin, and E. Stroup, Clin. Mater. **11**, 67 (1992).